https://doi.org/10.5194/tc-2020-92
Preprint. Discussion started: 21 April 2020

The Cryosphere Discussions
Open Access
EGU

Small scale spatial variability of bare-ice albedo at Jamtalferner, Austria

Lea Hartl[1], Lucia Felbauer[1], Gabriele Schwaizer[2], Andrea Fischer[1]

[1]Institute for Interdisciplinary Mountain Reasearch, Austrian Academy of Sciences, Technikerstraße, 21a, ICT, 6020 Innsbruck, Austria

[2]ENVEO GmbH, Fürstenweg 176, 6020 Innsbruck, Austria

Correspondence to: Lea Hartl (lea.hartl@oeaw.ac.at)

Abstract

As Alpine glaciers recede, they are quickly becoming snow free in summer and, accordingly, spatial and temporal variations in ice albedo increasingly affect the melt regime. To accurately model future developments, such as deglaciation patterns, it is important to understand the processes governing broadband and spectral albedo at a local scale. However, little in situ data of ice albedo exits. As a contribution to this knowledge gap, we present spectral reflectance data from 325 to 1075 nm collected along several profile lines in the ablation zone of Jamtalferner, Austria. Measurements were timed to closely coincide with a Sentinel 2 and Landsat 8 overpass and are compared to the respective ground reflectance products. The brightest spectra have a maximum reflectance of up to 0.7 and consist of clean, dry ice. In contrast, reflectance does not exceed 0.2 at dark spectra where liquid water and/or fine grained debris are present. Spectra can roughly be grouped into dry ice, wet ice, and dirt/rocks, although transitions between types are fluid. Neither satellite captures the full range of in situ reflectance values. The difference between ground and satellite data is not uniform across satellite bands, between Landsat and Sentinel, and to some extent between ice surface types (underestimation of reflectance for bright surfaces, overestimation for dark surfaces). We wish to highlight the need for further, systematic measurements of in situ spectral albedo, its variability in time and space, and in- depth analysis of time-synchronous satellite data.

1 Introduction

1.1 General context and aims

Under ongoing climate change, mountain glaciers are retreating at unprecedented rates (Zemp et al, 2015, 2019). Glaciers in the Eastern Alps are losing mass rapidly, and many have also lost their firn cover, so that darker bare ice is exposed. This in turn increases the amount of energy absorbed and accelerates melt (e.g. Paul et al., 2005; Box et al., 2012; Naegeli et al., 2017 & 2019). The magnitude and variability of albedo of glacier ice is affected by e.g. the absence or presence and amount of dust, pollen, debris, cryoconite, supraglacial water, and biota including local production rates. Variability is understood to

https://doi.org/10.5194/tc-2020-92
Preprint. Discussion started: 21 April 2020

be high, but few measurements and models exist. In a glaciological context, the spatial and temporal variability of ice albedo is understudied compared to snow albedo.

We present spectroradiometric data on the spatial variability of bare ice albedo at the tongue of Jamtalferner, Austria, aiming to contribute to closing the gap of knowledge in bare ice variability as an important feedback mechanism in glacier mass loss. Specifically, we aim to:

1) Provide a first-order quantitative assessment of spatial variability of surface reflectance in the ablation area of the rapidly melting Jamtalferner, quantifying possible ranges of spectral reflectance and qualitatively summarizing different surface types.
2) Compare commonly used, comparatively high resolution satellite-derived reflectance products with in situ measurements, highlighting areas in which further study is required if ongoing processes related to deglaciation are to be fully captured by satellite data.

1.2 In situ and remote sensing based change detection of surface reflectance

While it is generally understood that albedo is a major driving factor for the energy balance and radiative regime of glaciers, few studies discuss ice albedo and its variability at the local level. Early investigations of ice albedo were carried out by Sauberer in 1938. Building on this work, Sauberer and Dirmhirn (1951) showed that albedo is highly variable in time and space and strongly affects the radiation balance. They reported mean values of 0.37 for clean ice and 0.13 for dirty ice at Sonnblick glacier (Austria), a pronounced diurnal cycle of albedo related to refreezing of the surface, and influence of wind transported fine mineral dust. In another study based on measurements at Sonnblick, they highlighted that the collection of mineral dust in cryoconite holes affects albedo, as does liquid water, and showed a diurnal reduction of albedo of about 0.2 under clear sky conditions which they attribute to melt-freeze cycles on the ice surface (Sauberer and Dirmhirn, 1952). Jaffé (1960) also pointed out the importance of cryoconite and air content in the upper most ice layer for the radiative properties. Dirmhirn and Trojer (1955) presented a histogram-like curve of the frequency of different ice-albedo values measured on the tongue of Hintereisferner (Austria): Broadband ice albedo ranges from <0.1 to about 0.58, with a frequency maximum at 0.28. Similar to the results from Sonnblick, melt-related diurnal albedo variations were also found at Hintereisferner. In a detailed study of the radiation balance at Hintereisferner, Hoinkes and Wendler (1968) showed the importance of summer snow falls on albedo, as well as seasonal changes in ice albedo, and their significant contribution to ablation.

The spectral reflectance of bare ice areas of Alpine glaciers, how it changes over time, and the associated driving processes at the glacier surface have become of increasing scientific interest in relatively recent times, alongside the growing dominance of bare ice areas both compared to overall glacier area and in terms of glacier-wide mass- and energy balance. A number of studies attribute recent darkening of European glaciers to increased accumulation of mineral dust (e.g. Oerlemans

https://doi.org/10.5194/tc-2020-92
Preprint. Discussion started: 21 April 2020

et al., 2009, Azzoni et al., 2016) and black carbon (e.g. Painter et al., 2013, Gabbi et al., 2015). Similar findings have been reported from the Himalayas (e.g. Ming et al. 2012, 2015; Qu et al. 2014) and the Greenland ice sheet (Dumont et al., 2009). Some discussion remains as to whether the observed darkening is primarily due to the increase of bare ice areas compared to overall glacier area, or whether there is a darkening of the bare ice areas as such, and if so, whether bare ice areas are darkening due to local processes or large scale systemic change (e.g. Box et al., 2012; Alexander et al., 2014; Naegeli, 2019).

Different methodological approaches have been used to address specific changes in the surface characteristics of the ablation zone as they relate to changes in albedo and energy absorption across the electromagnetic spectrum: Using both hyperspectral satellite data and in situ measurements, Di Mauro et al. (2017) find that the presence of elemental and organic carbon leads to darkening of the ablation zone at Vadret da Morteratsch glacier (Switzerland) and discuss potential anthropogenic contributions. Azzoni et al. (2016) use semi-automatic image analysis techniques on photos of the ice surface at Forni glacier (Italy) to quantify the amount of fine debris present on the surface and its effect on the albedo. They find an overall darkening due to increasing dust, as well as significant effects of melt water.

Brun et al. (2015) highlight the importance of remote sensing data for monitoring of glacier albedo changes in remote regions and compare MODIS data with in situ radiation measurements. Naegeli et al. (2015) use in situ spectrometer and airborne image spectroscopy data to classify glacier surfaces types and map spectral albedo on Glacier de la Plaine Morte in Switzerland. Additionally, they highlight the difference in scale between albedo variability at the ice surface and the pixel resolution of satellite data and the need for detailed case studies combining ground truth data and remote sensing techniques to bridge this gap.

Naegeli et al. (2019) quantify trends in bare ice albedo for 39 Swiss glaciers using Landsat surface reflectance data products for a 17 year period. While they do not find a clear, wide spread darkening trend of bare ice surfaces throughout the entirety of their data set, they note significant negative trends at the local level, most notably for certain terminus areas. A detailed comparison of different albedo products derived from different kinds of remote sensing data (Landsat, Sentinel, APEX) by Naegeli et al. (2017) further highlights the gap between albedo variability on the ground and it's representation in remote sensing data of varying resolution.

Despite the growing body of work on this topic (see Table 1), reflectance – spectral as well as broadband - remains understudied compared to other parameters routinely recorded at Jamtalferner and other long-term glaciological monitoring sites. However, surface changes and associated changes of the spectral characteristics in the ablation area (e.g. due to debris cover, supraglacial meltwater, deposition of impurities) are expected to play a significant role in determining the future development of these glaciers. Incorporating relevant parameters into monitoring efforts is highly desirable. The accuracy of direct measurements of mass balance depends on the representation of all surface types in the stake network, and the correct

https://doi.org/10.5194/tc-2020-92
Preprint. Discussion started: 21 April 2020

attribution of unmeasured areas to measured stake ablation. Accordingly, a better understanding of surface albedo types is required to maintain the stake network on a rapidly changing glacier. To this end, it is important to understand whether satellite-derived data can provide a basis for defining surface albedo classes to be covered by stakes, or whether it does not allow for the retrieval of the full bandwidth of albedo variability relevant to the ice melt rate.

2. Data, Methods, and Study Site

2.1 Study site – glaciological background

Jamtalferner is located in the Silvretta mountain range, which intersects the border between Austria and Switzerland. Jamtalferner is the largest glacier on the Austrian side of Silvretta (Fig. 1, size in 1970: 4.115km², size in 2015: 2.818km²). The history of scientific research at the site goes back as far as 1892, when length change measurements were first carried out and a wealth of cartographic, geodetic, and glaciological data are available (Fischer et al., 2019). Orthophotos and cartographic analysis show that debris cover at the glacier terminus and in the lower elevation zones has increased (debris covered percentage of total area: 1.7% in 1970, 24.1% in 2015, Fig. 2 and 3), while firn cover is decreasing (firn covered area in 1970: 75%, in 2015: 13%, Fig. 2 and 3, Fischer et al., in review).

Mass balance measurements via the direct glaciological method began in 1988/1989. In recent years, increasing mass loss was recorded across all elevation zones (Fig. 3 Fischer et al., 2016; Fischer et al., in review). The lowest elevation zones are dominant in terms of total ablation and thus net balance. Melt in lowest altitudes has been increasing during the last two decades of negative mass balances and the variability of surface albedo at and near the glacier terminus affects melt over the full duration of the ablation season.

2.2 Ground measurements of spectral reflectance

Using a Field Spec Handheld 2 spectroradiometer, a total of 246 reflectance spectra was collected, with 12 spectra measured at point locations and 234 spectra measured along 16 profile lines. 14 profile lines contain 11 spectra, gathered at equal intervals between the start and end point of the profile, along a 20m measuring tape. 2 profiles contain 40 spectra – these were also gathered at equal intervals but with a higher resolution. The instrument operates between 325 and 1075 nm with an accuracy of ±1 nm and a resolution of <3 nm at 700 nm. For calibration, a new SRT-- 99-020 Spectralon (serial number 99AA08-0918-1593) manufactured by Lab Sphere was used. Initial processing of the raw ASD data files was carried out using the specdal Python package.

https://doi.org/10.5194/tc-2020-92
Preprint. Discussion started: 21 April 2020

2.3 Satellite data

We compare the ground measurements with surface reflectance products derived from a Landsat 8 Operational Land Imager (OLI) scene acquired on September 3rd, 2019 (10:10:32Z), the day before the ground measurements, and a Sentinel 2A scene acquired on September 4th, the same day as the ground measurements. Both scenes are cloud free over the study area. Details on the atmospheric correction algorithm used to generate the Landsat 8 OLI level-2 surface reflectance data product from top of atmosphere reflectance can be found in Vermote et al. (2016). Details on the equivalent Sentinel 2 product – the Level-2A bottom of atmosphere reflectance – are given in Main-Knorn et al. (2017). For the sake of readability, we refer to the Landsat 8 OLI level-2 surface reflectance as "Landsat" data in the following, and to the Sentinel 2A level-2A surface reflectance as "Sentinel" data. The Landsat and Sentinel surface reflectance raster data used in this study were acquired using google earth engine (Gorelick et al., 2017).

The wavelength range of the spectral reflectance measurements carried out on the ground overlaps with bands 1-5 of the Landsat data and bands 1-9 and 8A of the Sentinel data, respectively. Only spectral ranges covered by these bands are considered for this study. The wavelengths and resolution of the individual bands are given in Table 3. For each ground measurement point, band values were extracted from the satellite scenes at the overlaying pixel.

In order to compare the satellite values with ground data, we compute mean values for the subsets of the spectral reflectance curves measured on the ground that correspond to the Landsat and Sentinel bands, respectively. Data are then grouped into profile lines and/or different bands, the Pearson correlation is computed for ground- and corresponding satellite data, and further comparisons are carried out using standard statistical metrics.

3. Results

3.1 Surface measurements

The in situ measurements exhibit extreme differences in surface albedo depending on the characteristics of the surface. Figure 4 shows the spectra grouped into profiles, as well as mean, median, maximum, and minimum spectral reflectance per profile. P3 is the "brightest" profile, with the highest maximum (up to 0.7) and minimum (up to 0.2) values of all profiles. Profiles 2, 11, and 14 are the darkest profiles and all of their respective spectral reflectance remain below 0.2 at all measured wavelengths. Figure 5 shows the ice surface along profile lines 3 (brightest) and 11 (darkest) for a visual comparison. In P3, the surface is mainly comprised of clean, dry ice. In P11, the ice surface is wet and impurities (rocks, fine grained debris) are present. The profile line crosses several small melt water channels with running water.

https://doi.org/10.5194/tc-2020-92
Preprint. Discussion started: 21 April 2020

Table 2 contains a qualitative description of the ice surface along each profile line, the length of the line, the number of spectra per line, and the number of Landsat and Sentinel band 3 pixels that each line crosses. The maximum number of pixels per line is 5 for Sentinel and 3 for Landsat, respectively. All lines cross at least 2 pixels for Sentinel, while 3 lines fall into a single Landsat pixel. See Fig. 1 for the location of each profile on the glacier.

The spectral reflectance curves of the individual spectra as well as of the profile lines indicate high spatial variation of surface types and associated reflective properties. The spectral signatures of the individual spectra can roughly be grouped into dry ice, wet ice, and dirt/rocks. (We use the word “dirt” to describe all types of mineral or organic materials and fine-grained debris that may collect on the glacier surface.) However, transitions between these types are fluid and in practice these categories cannot always be clearly separated - both dry and wet ice might be clean or dirty, dirt might be wet or dry.

The reflectance curves for clean ice exhibit the typical shape frequently found in literature (Zeng et al., 1984), with highest reflectance values (up to 0.69) in the lower third of our wavelength range and declining values for wavelengths greater than approximately 580 nm. The spectral reflectance curves of wet ice surfaces follow roughly the same shape as for dry ice but are strongly dampened in amplitude with reflectance values typically not exceeding 0.2. In contrast, the reflectance curve of dirty surfaces remains at uniformly low values throughout our wavelength range in some cases and exhibits an increase between 325 and approximately 550 nm before flattening out in other cases. Reflectance values have similar magnitudes as for wet ice. Example reflectance curves of these surface types are given in Fig. 6.

3.2 Comparison with satellite data

Figure 7 shows all measured spectral reflectance curves, as well as the Sentinel and Landsat values in the bands that overlap the wavelength range of the ground measurements. The satellite values in the figure are the values extracted from the Sentinel and Landsat pixels, respectively, for each ground measurement point. Naturally, neither satellite captures the full range of reflectance values measured on the ground. In all overlapping bands of Sentinel and Landsat, the Sentinel values are higher, in the sense that the maximum values of the Sentinel data are closer to the maximum values measured on the ground, while the minimum Landsat data are closer to the minimum values measured on the ground.

Comparing the mean of the spectral reflectances measured on the ground for each satellite band with the associated satellite values yields a Pearson correlation coefficient ranging from 0.53 (band 5) to 0.62 (band 1) for the Landsat bands and 0.3 (band 9) to 0.65 (band 2) for Sentinel. Table 3 lists the correlation coefficients, as well as the wavelength range and resolution of each band. The two lower resolution Sentinel bands (band 1, band 9 – 60m resolution) have notably lower correlation coefficients than the higher resolution bands. The Sentinel and Landsat data at the ground measurement points are strongly correlated with each other in the bands where both satellites overlap, with $r=0.69$ in band 1 and $r>0.8$ for bands 2, 3, 4, and 5.

https://doi.org/10.5194/tc-2020-92
Preprint. Discussion started: 21 April 2020

For a visual comparison of the location of the profile lines and the range of measured values in the profiles in relation to the satellite pixel boundaries and pixel band values, see Fig. 8 for Sentinel (band 3 selected as an example) and supplementary material for an analogous figure of the Landsat data.)

The spread of ground reflectance values per profile is generally lower for profiles that are darker overall, and greater for brighter profiles, although not in all cases (Fig.4, Fig. 9). In the Sentinel band 3 wavelength range, profile 3 is brightest with a median reflectance of 0.48 and spread of 0.49. Profile 6 (median reflectance in Sentinel band 3 range: 0.21) has the largest spread of reflectances (0.52). Broadly speaking, profiles with a high median reflectance tend to include individual measurement points that are both very bright and very dark, while darker profiles are more uniformly dark. Profile 6 in particular transitions between surface types and contains wet/dirty spectra as well as dry ice spectra (see Table 2). Figure 9 shows boxplots of the ground measurements (band 3 mean) for all profiles to exemplify this and indicates where the Landsat and Sentinel values fall compared to the spread of values in each profile.

When binning ground measurements by the associated satellite value/pixel and taking the median or mean of the binned values, the difference between the median/mean ground value and the satellite value tends to decrease with increasing number of ground measurements mapped to unique satellite values. This is to be expected, as each satellite value represents an integration of the emission characteristics over the area contained in the pixel. However, for our data, this relationship is not obviously linear and differs between Sentinel and Landsat, as well as between different bands (Figure 10).

Comparing ground and satellite values for individual ground measurement points, it is apparent that both satellites tend to overestimate the reflectance values of dark ground surfaces, and underestimate the reflectance of bright surfaces, in all bands (Figure 11). The shift from over- to underestimation appears linear and has a similar increase rate in all bands. The zero crossings of the regression lines, i.e. the ground reflectance values for which ground measurements and satellite values match, fall between 0.15 (band 5) and 0.21 (band 1) for Landsat and 0.17 (band 9) and 0.27 (band 3) for Sentinel.

Figure 12 shows histograms of the mean reflectance in band 3 of Landsat and Sentinel, respectively, compared with associated in situ values, as well as density plots over reflectance over all pixels in the study area. The mean is highest in the in situ measurements and lowest in Landsat images. Both Sentinel and Landsat fail to capture reflectances below 0.05 and above 0.45. A second peak in frequency evident from the in situ measurements at a reflectance of 0.4 is not represented in the remote sensing data.

https://doi.org/10.5194/tc-2020-92
Preprint. Discussion started: 21 April 2020

4. Discussion

The different surface types identified at Jamtalferner (Fig. 6) and their spectral reflectances are comparable to types of surfaces identified in Switzerland at Morteratsch and Glacier de la Plaine Morte by Di Mauro et al. (2017) and Naegeli et al. (2015), respectively, supporting the use of a classification scheme based on differentiating between a) clean and dirty ice surfaces and b) the presence or absence of liquid water on the ice surface. It is generally understood that both "dirt" (organic or inorganic impurities) and liquid water reduce the reflectance of ice (e.g. Hall, 2012) and early studies showed diurnal cycles and high spatial variability of broadband albedo (Sauberer and Dirmhirn, 1951 & 1951; Dirmhirn and Trojer, 1955). However, understanding of how and why spectral ice albedo changes in time and space and how this affects the amount of energy available for melt remains incomplete.

High resolution time series of spectral reflectance at representative locations in the ablation zone are needed to assess how changes in wetness and temperature, surface texture (cryoconite formation, roughness changes during the season), biotic productivity and erosion and deposition of sediment by melt water and rain affect albedo on a small spatial scale, throughout the day and over the course of the ablation season. Establishing measurement efforts aimed at generating such time series on glaciers with existing mass balance monitoring networks would be highly desirable.

In order to scale assessments of ice albedo from the local to a regional or global level, satellite-derived data are indispensable. Earlier in the satellite era, several studies carried out comparisons of albedo data measured on the ground and surface reflectance derived from Landsat 5 Thematic Mapper scenes, finding considerable differences between in situ and satellite data especially in the ablation area (e.g. Hall et al., 1989 & 1990; Koelemeijer et al., 1993; Winther, 1993; Knap et al., 1999). These works are mostly based on albedo data from a single location, such as a weather station, and it was often not possible to carry out ground measurements so that they coincided with the satellite overpasses.

In more recent studies, an increasing focus is given to narrow-to-broadband conversions (Gardner et al, 2010; Naegeli et al., 2017). However, commonly used conversions are typically designed for use with Landsat 5 or 7, rather than Landsat 8 or Sentinel 2, which increases the challenges and uncertainties inherently associated with any narrow-to-broadband conversion. In addition, studies assessing the potential effects of anisotropy on satellite-derived surface reflectance data are sparse and the magnitude of associated uncertainties is hard to quantify (Naegeli et al., 2015 & 2017).

In comparing our in situ measurements with readily available L2A satellite products, we chose an "as simple as possible" approach to gain a general understanding of where sources of uncertainties are. The albedo variability on the ground is not fully represented in the satellite data, which raises questions as to how well surface processes at rapidly changing glaciers

https://doi.org/10.5194/tc-2020-92
Preprint. Discussion started: 21 April 2020

such as Jamtalferner can be resolved with satellite data. Surface reflectance products might be improved by developing dedicated atmospheric correction algorithms and quantifying the influence of anisotropy and different narrow-to-broadband conversions. Systematic collection of ground truth data will be fundamental to assessing the potential range and variations of uncertainty in satellite derived glacier ice albedo and potentially reducing this uncertainty.

In addition to albedo, other feedback mechanisms such as changing topography and glacier geometry, also significantly impact the rate of glacial retreat, contributing to the non-linear characteristics of glacier change and the high variability of defining parameters such as mass-balance or area change even among neighbouring glaciers subject to common climatic drivers (Charalampidis et al., 2018). Understanding these feedback mechanisms and associated processes is key to successfully predicting future glacier changes across spatial and temporal scales. Ice albedo will remain a significant source of uncertainty as long as the processes governing temporal and spatial variability are not fully understood.

5. Conclusion & Outlook

Our comparatively simplistic statistical comparison of Landsat and Sentinel L2A products with in situ data serves to exemplify that the difference between ground and satellite data is not uniform across satellite bands, between Landsat and Sentinel, and to some extent between ice surface types (underestimation of reflectance for bright surfaces, overestimation for dark surfaces). Assessing the reasons for these differences – with the eventual goal of improving satellite-derived surface reflectance of glacier ice – requires 1) further, systematic measurements of in situ spectral albedo and 2) in depth analysis of time-synchronous satellite data.

Given that increasing debris cover is already observed to be an major unknown during glacier disintegration and even deglaciation (e.g. Fischer et al., 2016; Fischer et al., in review), we urgently need to improve our process understanding and our data basis regarding albedo changes on glaciers. Quantifying spatial and temporal variability of spectral reflectance and delineating the main causes of this variability for individual glaciers will improve modelling capabilities of glacier evolution and catchment hydrology. Satellite-derived reflectance products are a key component of tackling similar questions on the regional and global level. However, ground truth data from representative sites is essential in order to understand uncertainties associated with satellite albedo products and potentially improve them for specific contexts.

Moving forward, an expansion of the monitoring network at Jamtalferner and, ideally, other glaciers, by continuous reflectance measurements in the ablation zone at a fixed location is needed, as well as “snap-shot” measurements of spectral reflectance at multiple strategic points in regular intervals. Combining analysis of spectral reflectance data from in situ and remote sensing sources with the wealth of contextual information available at Jamtalferner and other established monitoring

https://doi.org/10.5194/tc-2020-92
Preprint. Discussion started: 21 April 2020

sites has the potential to greatly improve our understanding of the complex interplay of surface changes, glacier dynamics, and mass- and energy balance.

Author Contribution

L. Felbauer and A. Fischer collected the in situ data. Subsequent data curation was carried out by L. Felbauer and L. Hartl. G. Schwaizer conceptualized the comparison of in situ and satellite derived data. L. Hartl developed the code for data analysis and visualizations, and wrote the manuscript with contributions from all co-authors.

Competing interests

The authors have no competing interests to declare.

Data availability

The spectral reflectance data was submitted to the data repository pangaea.de and the DOI of the data set will be cited in the final version of this publication once it becomes available.

Acknowledgements

We are very grateful to Gottlieb Lorenz and the entire team at the Jamtal Hütte for providing an excellent base for field work at Jamtalferner and invaluable support over the years.

References

Alexander, P. M., Tedesco, M., Fettweis, X., Van De Wal, R., Smeets, C. J. P. P., and Van Den Broeke, M. R.: Assessing spatio-temporal variability and trends in modelled and measured Greenland Ice Sheet albedo (2000-2013), The Cryosphere, 8(6), 2293-2312, 2014.

Azzoni, R. S., Senese, A., Zerboni, A., Maugeri, M., Smiraglia, C., and Diolaiuti, G. A.: Estimating ice albedo from fine debris cover quantified by a semi-automatic method: the case study of Forni Glacier, Italian Alps, The Cryosphere, 10, 665-679, 2016.

Box, J. E., Fettweis, X., Stroeve, J. C., Tedesco, M., Hall, D. K., and Steffen, K.: Greenland ice sheet albedo feedback: thermodynamics and atmospheric drivers, The Cryosphere, 6(4), 821-839, 2012.

https://doi.org/10.5194/tc-2020-92
Preprint. Discussion started: 21 April 2020

Brun, F., Dumont, M., Wagnon, P., Berthier, E., Azam, M. F., Shea, J. M., Sirguey, P., Rabatel, A., and Ramanathan, A.: Seasonal changes in surface albedo of Himalayan glaciers from MODIS data and links with the annual mass balance, The Cryosphere, 9(1), 341-355, 2015.

Charalampidis, C., Fischer, A., Kuhn, M., Lambrecht, A., Mayer, C., Thomaidis, K., and Weber, M.: Mass-budget anomalies and geometry signals of three Austrian glaciers, Frontiers in Earth Science, 6, p. 218, 2018.

Dirmhirn, I. and Trojer, E.: Albedountersuchungen auf dem Hintereisferner, Archiv für Meteorologie, Geophysik und Bioklimatologie, Serie B, 6(4), pp.400-416, 1955.

Dumont, M., Brun, E., Picard, G., Michou, M., Libois, Q., Petit, J. R., Geyer, S., and Josse, B.: Contribution of light-absorbing impurities in snow to Greenland's darkening since 2009, Nature Geoscience, 7(7), 509, 2014.

Fischer, A., Helfricht, K., Wiesenegger, H., Hartl, L., Seiser, B., and Stocker-Waldhuber, M.: Chapter 9 - What Future for Mountain Glaciers? Insights and Implications From Long-Term Monitoring in the Austrian Alps, in: Developments in Earth Surface Processes, edited by: Greenwood, G., B. and Shroder, J. F., Elsevier, 21, 325-382, 2016.

Fischer, A., Markl, G., and Kuhn, M.: Glacier mass balances and elevation zones of Jamtalferner, Silvretta, Austria, 1988/1989 to 2016/2017, Institut für Interdisziplinäre Gebirgsforschung der Österreichischen Akademie der Wissenschaften, Innsbruck, PANGAEA, https://doi.org/10.1594/PANGAEA.818772, 2016.

Fischer, A., Fickert, T., Schwaizer, G., Patzelt, G. and Groß, G.: Vegetation dynamics in Alpine glacier forelands tackled from space, Scientific reports, 9(1), pp.1-13, 2019.

Fischer, A., Seiser, B., and Stocker-Waldhuber, M.: Capturing deglaciation in the Austrian Silvretta: Methods and Results, in review.

Gabbi, J., Huss, M., Bauder, A., Cao, F., & Schwikowski, M.: The impact of Saharan dust and black carbon on albedo and long-term mass balance of an Alpine glacier, The Cryosphere, 9(4), 1385-1400, 2015.

Gardner, A. S. and Sharp, M. J.: A review of snow and ice albedo and the development of a new physically based broadband albedo parameterization, Journal of Geophysical Research: Earth Surface, 115(F1), 2010.

Gorelick, N., Hancher, M., Dixon, M., Ilyushchenko, S., Thau, D., and Moore, R.: Google Earth Engine: Planetary-scale geospatial analysis for everyone, Remote Sensing of Environment, 202, pp.18-27, 2017.

Jaffé, A.: Über Strahlungseigenschaften des Gletschereises, Archiv für Meteorologie, Geophysik und Bioklimatologie, Serie B, 10(3), pp.376-395, 1960.

Knap, W. H., Brock, B. W., Oerlemans, J., and Willis, I. C.: Comparison of Landsat TM-derived and ground-based albedos of Haut Glacier d'Arolla, Switzerland, International Journal of Remote Sensing, 20(17), 3293-3310, 1999.

Koelemeijer, R., Oerlemans, J., and Tjemkes, S.: Surface reflectance of Hintereisferner, Austria, from Landsat 5 TM imagery, Annals of Glaciology, 17, 17-22, 1993,

Kuhn, M.: The response of the equilibrium line altitude to climate fluctuations: theory and observations, in: Glacier fluctuations and climatic change, 407-417, Springer, Dordrecht, 1989.

https://doi.org/10.5194/tc-2020-92
Preprint. Discussion started: 21 April 2020

Hall, D. K., Chang, A. T. C., Foster, J. L., Benson, C. S., and Kovalick, W. M.: Comparison of in situ and Landsat derived reflectance of Alaskan glaciers, Remote Sensing of Environment, 28, 23-31, 1989.

Hall, D. K., Bindschadler, R. A., Foster, J. L., Chang, A. T. C., and Siddalingaiah, H.: Comparison of in situ and satellite-derived reflectances of Forbindels Glacier, Greenland, Remote Sensing, 11(3), 493-504, 1990.

Hall, D.: Remote sensing of ice and snow, Springer Netherlands, 2012.

Hoinkes, H., and Wendler, G.: Der Anteil der Strahlung an der Ablation von Hintereis-und Kesselwandferner (Ötztaler Alpen, Tirol) im Sommer 1958, Archiv für Meteorologie, Geophysik und Bioklimatologie, Serie B, 16(2-3), 195-236, 1968.

Main-Knorn, M., Pflug, B., Louis, J., Debaecker, V., Müller-Wilm, U., and Gascon, F.: Sen2Cor for Sentinel-2, in: Image and Signal Processing for Remote Sensing XXIII, International Society for Optics and Photonics, Warsaw, Poland, 11-13 September 2017, Vol. 10427, p. 1042704, 2017.

Di Mauro, B., Baccolo, G., Garzonio, R., Giardino, C., Massabò, D., Piazzalunga, A., Rossini, M., and Colombo, R.: Impact of impurities and cryoconite on the optical properties of the Morteratsch Glacier (Swiss Alps), The Cryosphere, 11(6), 2393, 2017.

Ming, J., Du, Z., Xiao, C., Xu, X., and Zhang, D.: Darkening of the mid-Himalaya glaciers since 2000 and the potential causes, Environmental Research Letters, 7(1), 014021, 2012.

Ming, J., Wang, Y., Du, Z., Zhang, T., Guo, W., Xiao, C., Xu, X., Ding, M., Zhang, D., and Yang, W.: Widespread albedo decreasing and induced melting of Himalayan snow and ice in the early 21st century, PLoS One, 10(6), e0126235, 2015.

Naegeli, K., Damm, A., Huss, M., Schaepman, M., & Hoelzle, M.: Imaging spectroscopy to assess the composition of ice surface materials and their impact on glacier mass balance, Remote Sensing of Environment, 168, 388-402, 2015.

Naegeli, K., Damm, A., Huss, M., Wulf, H., Schaepman, M., & Hoelzle, M.: Cross-Comparison of albedo products for glacier surfaces derived from airborne and satellite (Sentinel-2 and Landsat 8) optical data, Remote Sensing, 9(2), 110, 2017.

Naegeli, K., Huss, M., & Hoelzle, M.: Change detection of bare-ice albedo in the Swiss Alps, The Cryosphere, 13(1), 397-412, 2019.

Oerlemans, J.: Glaciers and climate change. CRC Press, 2001.

Oerlemans, J., R. H. Giesen, and M. R. Van den Broeke: Retreating alpine glaciers: increased melt rates due to accumulation of dust (Vadret da Morteratsch, Switzerland), Journal of Glaciology, 55, no. 192, 729-736, 2009.

Painter, T. H., Flanner, M. G., Kaser, G., Marzeion, B., VanCuren, R. A., and Abdalati, W.: End of the Little Ice Age in the Alps forced by industrial black carbon, Proceedings of the National Academy of Sciences, 110(38), 15216-15221, 2013.

Paul, F., Machguth, H., and Kääb, A.: On the impact of glacier albedo under conditions of extreme glacier melt: the summer of 2003 in the Alps, EARSeL eProceedings,4(2), 139-149, 2005.

Qu, B., Ming, J., Kang, S. C., Zhang, G. S., Li, Y. W., Li, C. D., Zhao, S.Y., Ji, Z. M., and Cao, J. J.: The decreasing albedo of the Zhadang glacier on western Nyainqentanglha and the role of light-absorbing impurities, Atmospheric Chemistry and Physics, 14(20), 11117-11128, 2014.

https://doi.org/10.5194/tc-2020-92
Preprint. Discussion started: 21 April 2020

Sauberer, F.: Versuche über spektrale Messungen der Strahlungseigenschaften von Schnee und Eis mit Photoelementen, Meteorol. Z., 55, 250, 1938.

Sauberer, F. and Dirmhirn, I.: Untersuchungen über die Strahlungsverhältnisse auf den Alpengletschern, Archiv Met. Geoph. Biokl. Ser. B.3, 256, 1951.

Sauberer, F. And Dirmhirn, I.: Der Strahlungshaushalt horizontaler Gletscherflächen auf dem Hohen Sonnblick, Geogr. Ann., 34, 261, 1952.

Van de Wal, R.S.W., Oerlemans, J., and Van der Hage, J.C.: A study of ablation variations on the tongue of Hintereisferner, Austrian Alps, Journal of Glaciology, 38(130), pp.319-324, 1992.

Vermote, E., Justice, C., Claverie, M., and Franch, B.: Preliminary analysis of the performance of the Landsat 8/OLI land surface reflectance product, Remote Sensing of Environment, 185, 46-56, 2016.

Winther, J. G.: Landsat TM derived and in situ summer reflectance of glaciers in Svalbard, Polar Research,12(1), 37-55, 1993.

Zemp, M., Frey, H., Gärtner-Roer, I., Nussbaumer, S.U., Hoelzle, M., Paul, F., Haeberli, W., Denzinger, F., Ahlstrøm, A.P., Anderson, B., and Bajracharya, S.: Historically unprecedented global glacier decline in the early 21st century, Journal of Glaciology, 61(228), pp.745-762, 2015.

Zemp, M., Huss, M., Thibert, E., Eckert, N., McNabb, R., Huber, J., Barandun, M., Machguth, H., Nussbaumer, S.U., Gärtner-Roer, I. and Thomson, L.: Global glacier mass changes and their contributions to sea-level rise from 1961 to 2016, Nature, 568(7752), pp.382-386, 2019.

Zeng, Q., Cao, M., Feng, X., Liang, F., Chen, X., and Sheng, W.: A study of spectral reflection characteristics for snow, ice and water in the north of China, Hydrological applications of remote sensing and remote data transmission, 145, pp.451-462, 1984.

https://doi.org/10.5194/tc-2020-92
Preprint. Discussion started: 21 April 2020

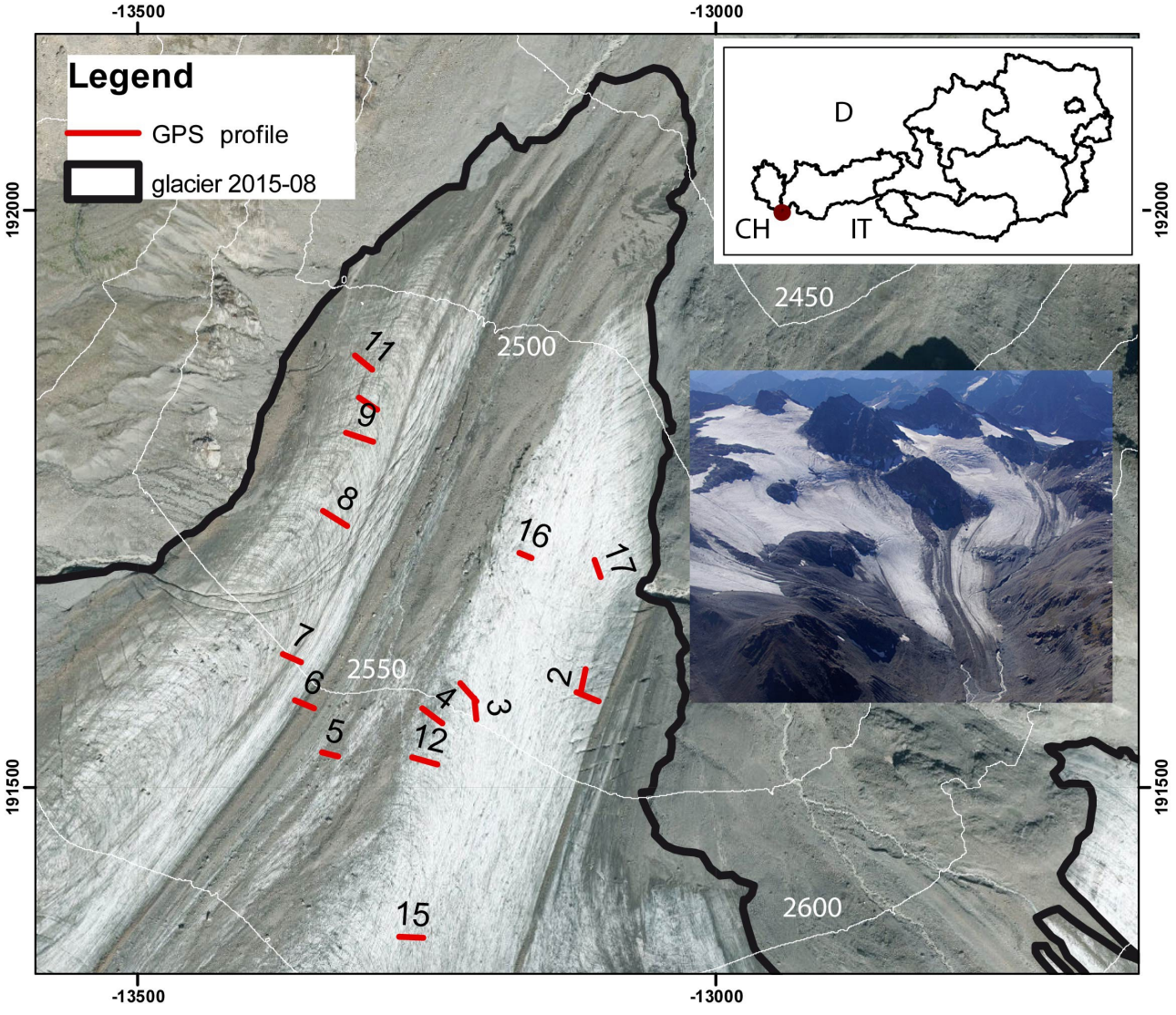

395 **Figure 1: Tongue of Jamtalferner glacier (Orthophoto, August 2015, Source: Tyrolean Government/ TIRIS) with profile lines of spectroadiometer measurements indicated in red. Insert: Areal photograph of Jamtalferner, 20.09.2018 (Photo: Andrea Fischer).**

https://doi.org/10.5194/tc-2020-92
Preprint. Discussion started: 21 April 2020

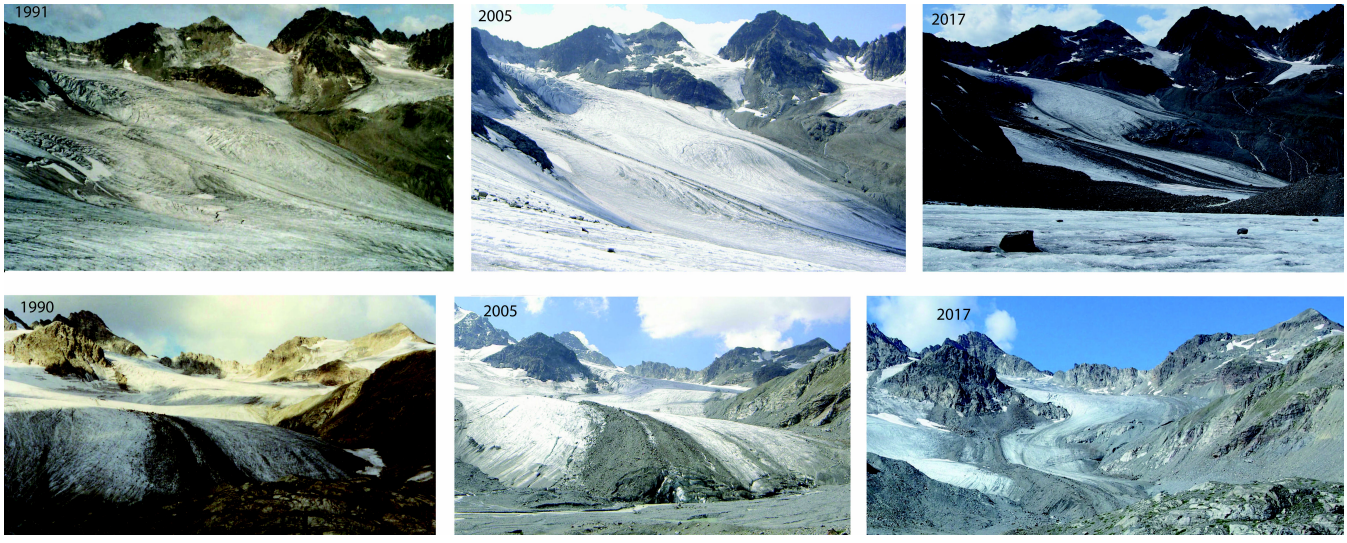

Figure 2: The upper part of the ablation zone of Jamtalferner (top panel) and the terminus (bottom panel) in the early 1990s (Photos: Gerhard Markl), 2005 and 2017 (Photos: Andrea Fischer).

https://doi.org/10.5194/tc-2020-92
Preprint. Discussion started: 21 April 2020

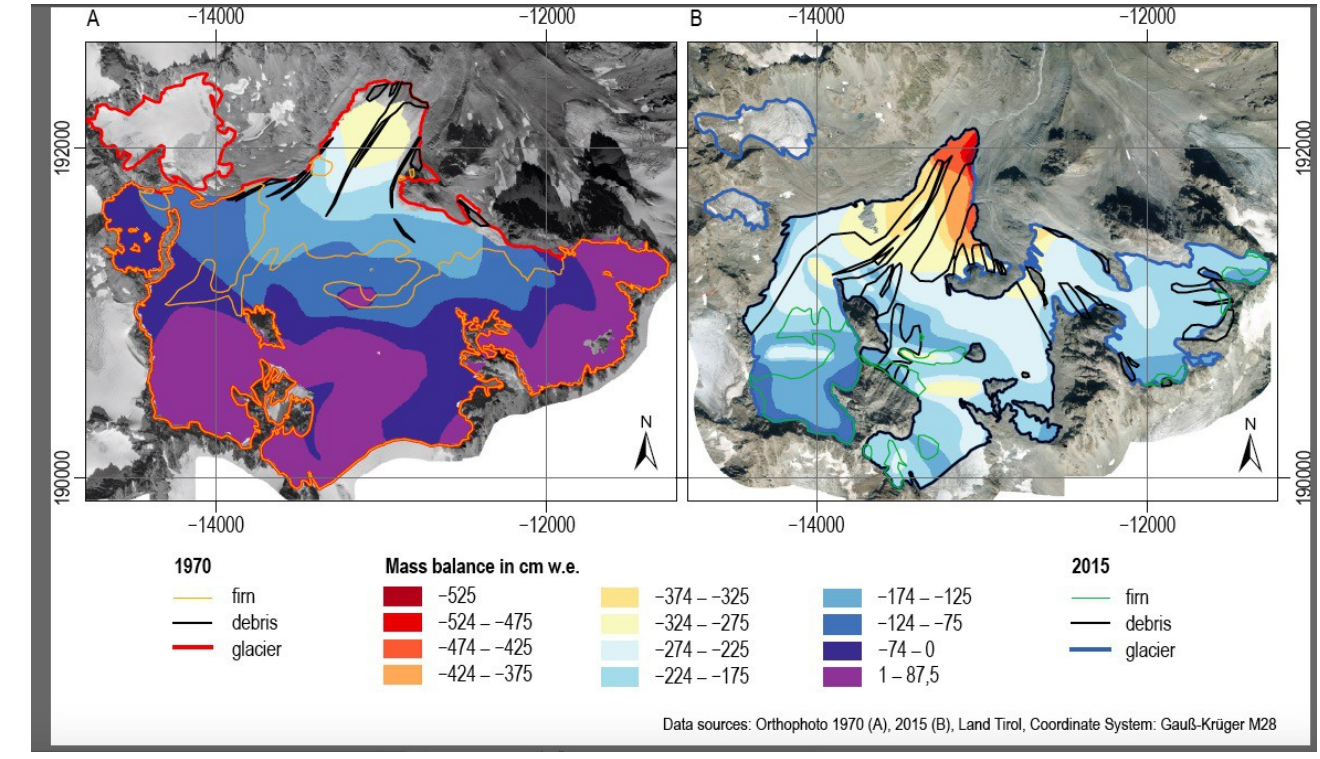

405

Figure 3: Outlines indicate summer firn coverage, bare ice areas, and debris cover in 1970 (left) and 2015 (right). Coloured areas show mass balance in cm water equivalent. in 1988/89 (first year of mass balance measurements at Jamtalferner) and the extremely negative mass balance year 2014/15. Background imagery: Orthophotos 1970 (A), 2015 (B), Tyrolean government.

https://doi.org/10.5194/tc-2020-92
Preprint. Discussion started: 21 April 2020

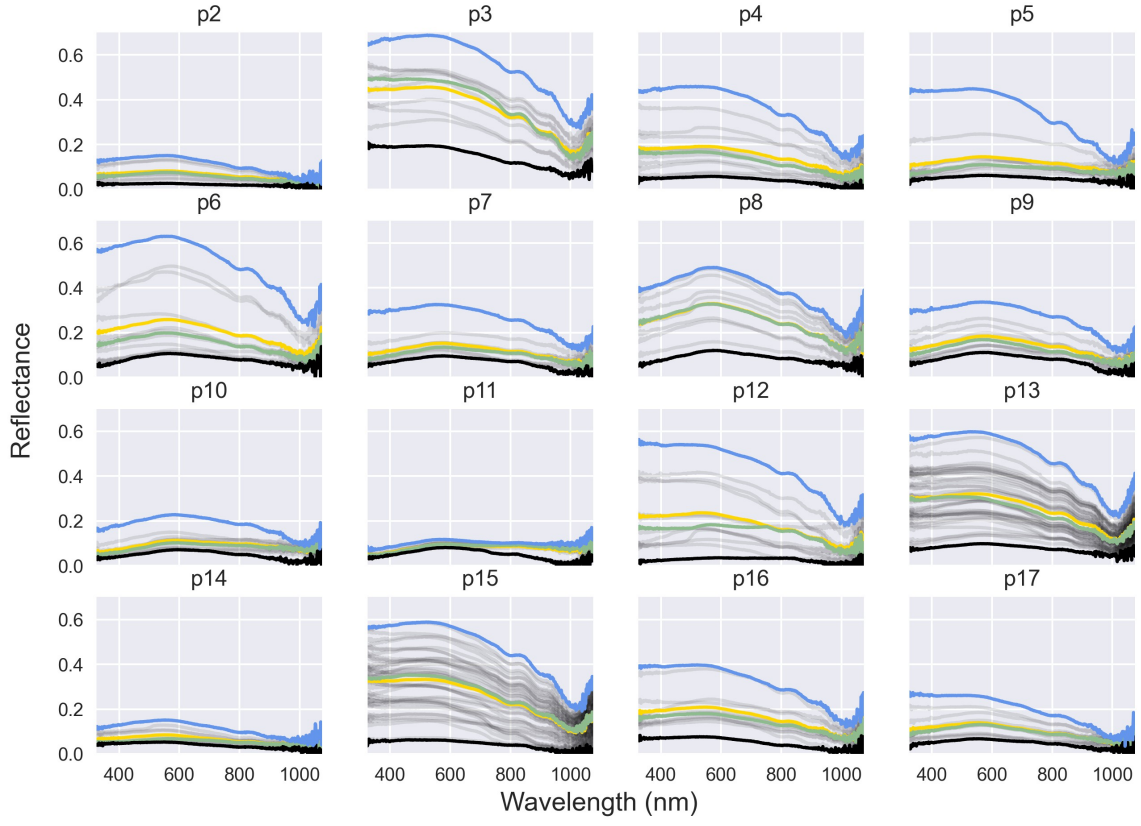

Figure 4: Each subplot shows the spectra along a profile line. The mean, median, maximum, and minimum spectral reflectance in each profile are highlighted in yellow, green, blue, black, respectively.

https://doi.org/10.5194/tc-2020-92
Preprint. Discussion started: 21 April 2020

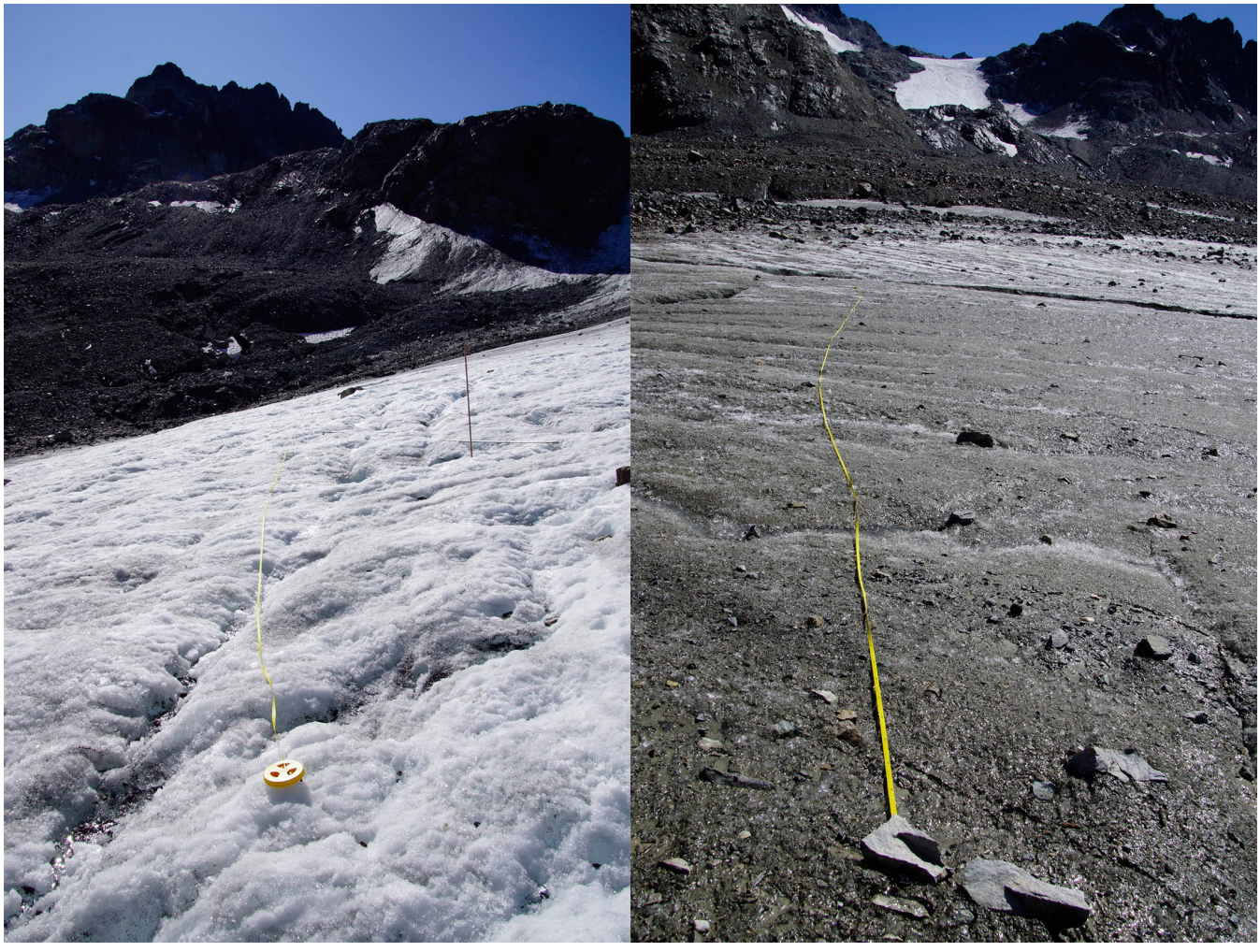

Figure 5: Photos of the ice surface along profile 3 (left) and profile 11 (right), at the time of measurement (Photo: Andrea Fischer).

https://doi.org/10.5194/tc-2020-92
Preprint. Discussion started: 21 April 2020

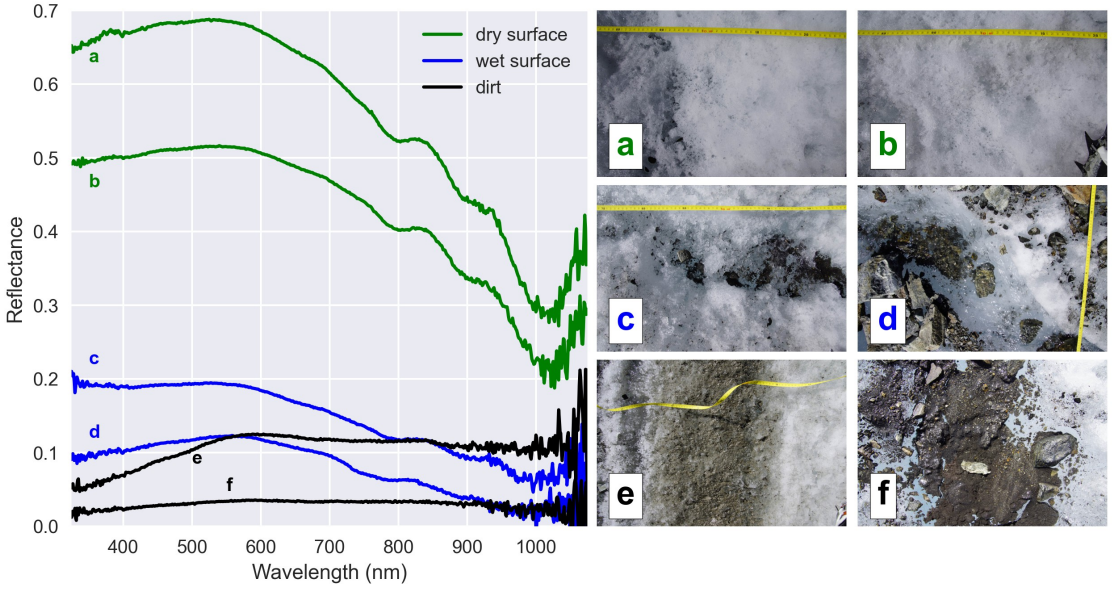

415 **Figure 6: Spectra of different kinds of ice surface types encountered in the ablation zone of Jamtalferner. The photos on the right show the ice surface at the sampling sites of the respective spectra. The spectra shown in this figure are part of the following profile lines: a, b, c – p3; d – p4; e – p6; f – p12.**

https://doi.org/10.5194/tc-2020-92
Preprint. Discussion started: 21 April 2020

The Cryosphere
Discussions
Open Access
EGU

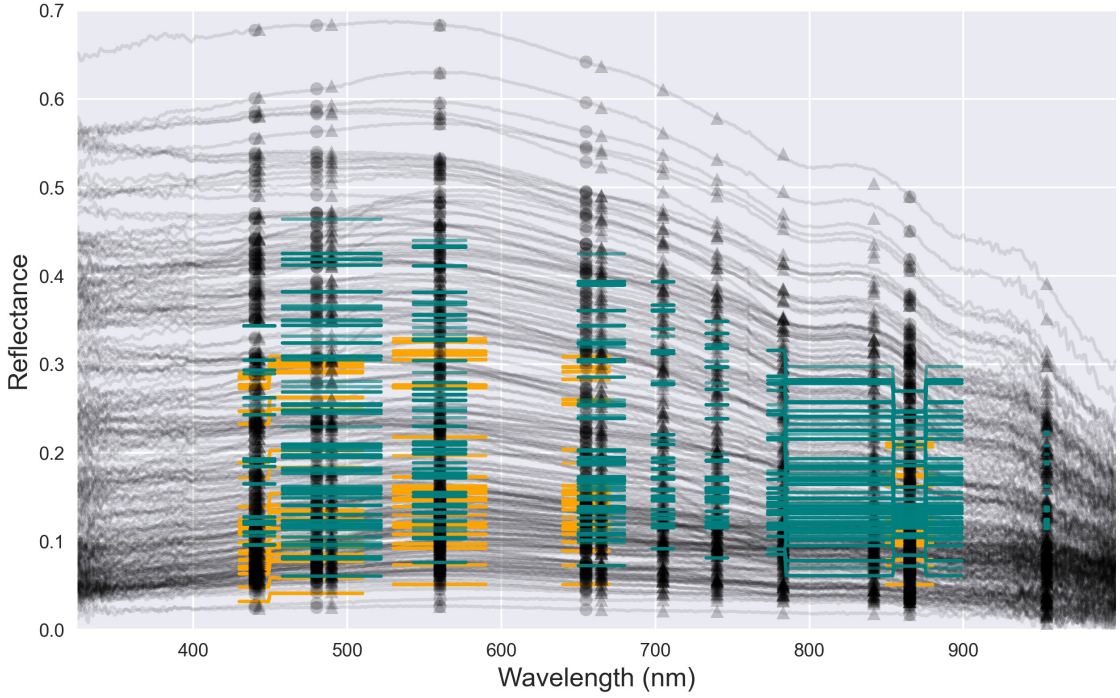

Figure 7: Spectra measured on the ground are plotted in black. Orange and blue lines represent the mean reflectance of all ground measurements in the wavelength range of the Landsat and Sentinel bands listed in Table 3. Black circles indicate the central wavelengths of the Landsat bands, black triangles those of the Sentinel bands.

https://doi.org/10.5194/tc-2020-92
Preprint. Discussion started: 21 April 2020

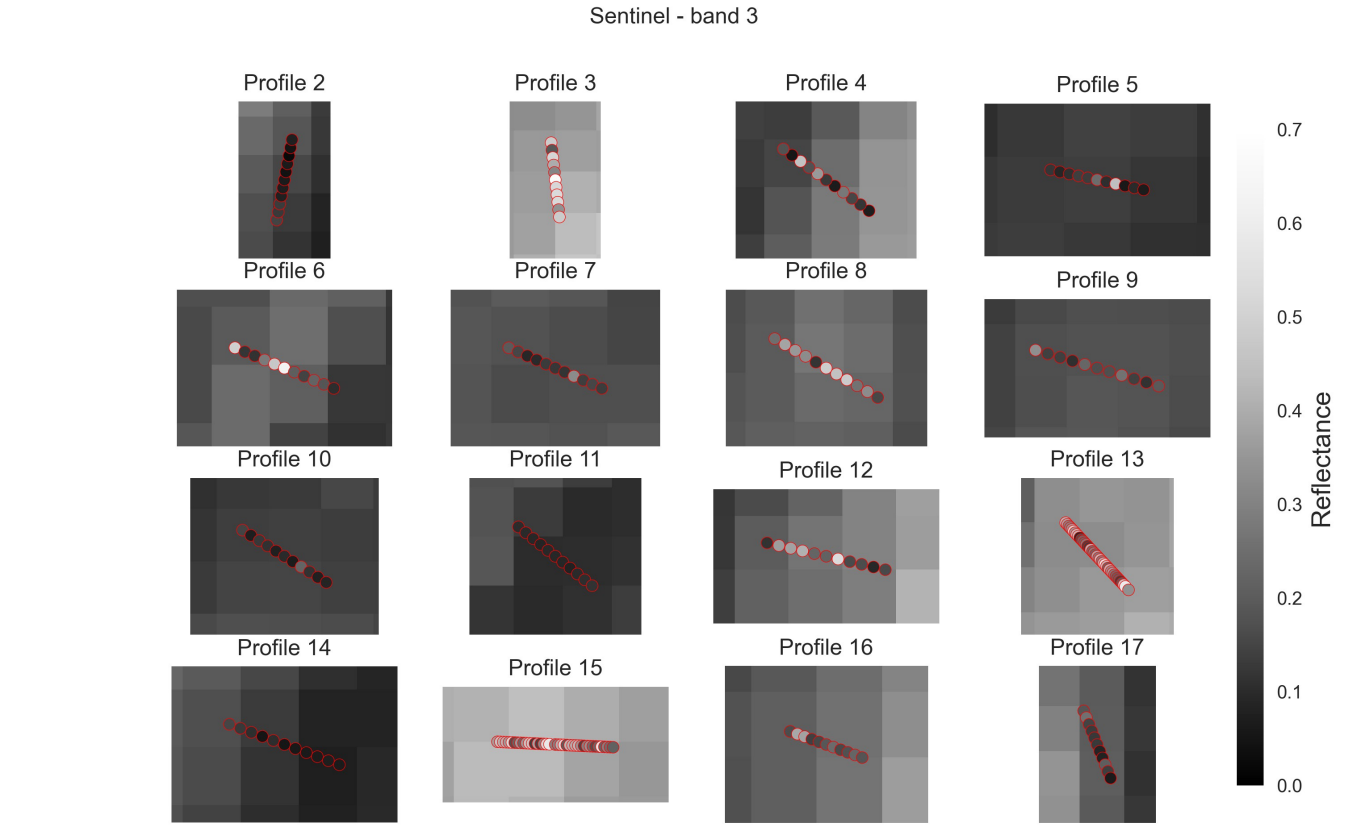

Figure 8: The spectra comprising the profile lines are plotted over the corresponding satellite pixels. The colour bar is the same for the background raster and the circles indicating the sampling sites of the spectra and represents the Sentinel band 3 pixel value and the mean reflectance in the Sentinel band 3 wavelength range of each spectrum, respectively.

https://doi.org/10.5194/tc-2020-92
Preprint. Discussion started: 21 April 2020

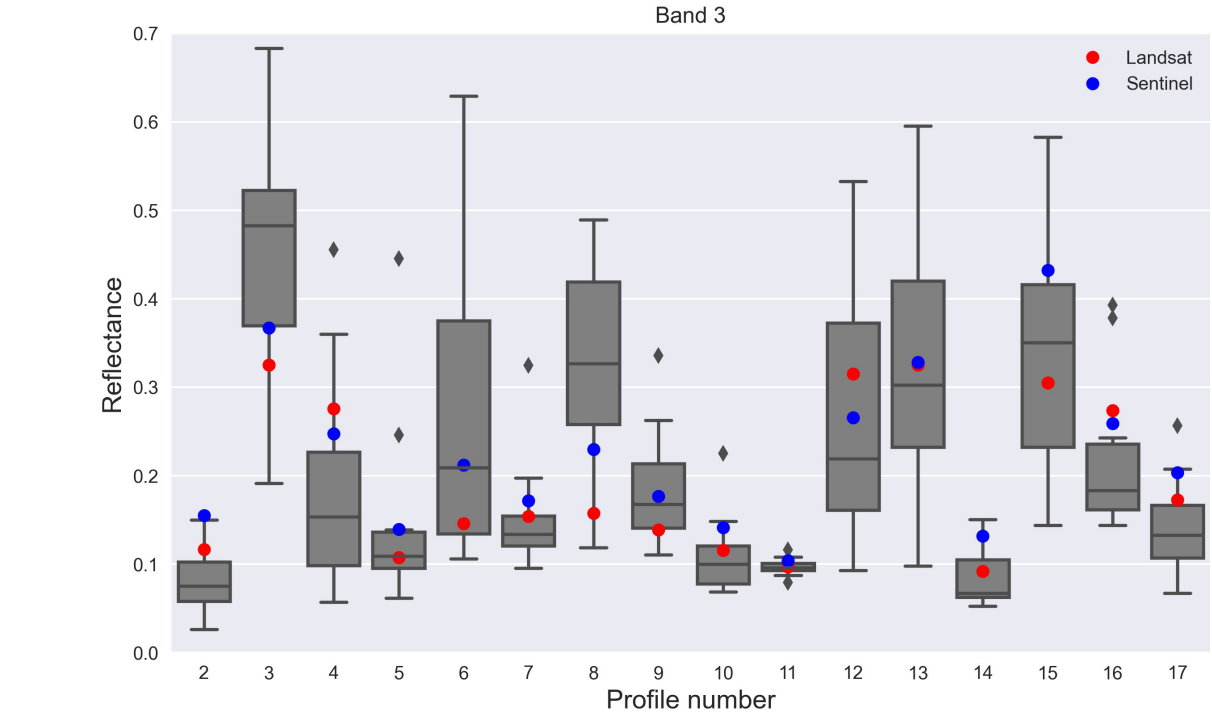

Figure 9: Spread of the band 3 (Sentinel wavelength range) mean values of the measured spectra, grouped by profile. Red and blue circles show corresponding mean pixel values of data extracted from Landsat and Sentinel pixels at the sampling sites of the spectra, respectively.

https://doi.org/10.5194/tc-2020-92
Preprint. Discussion started: 21 April 2020

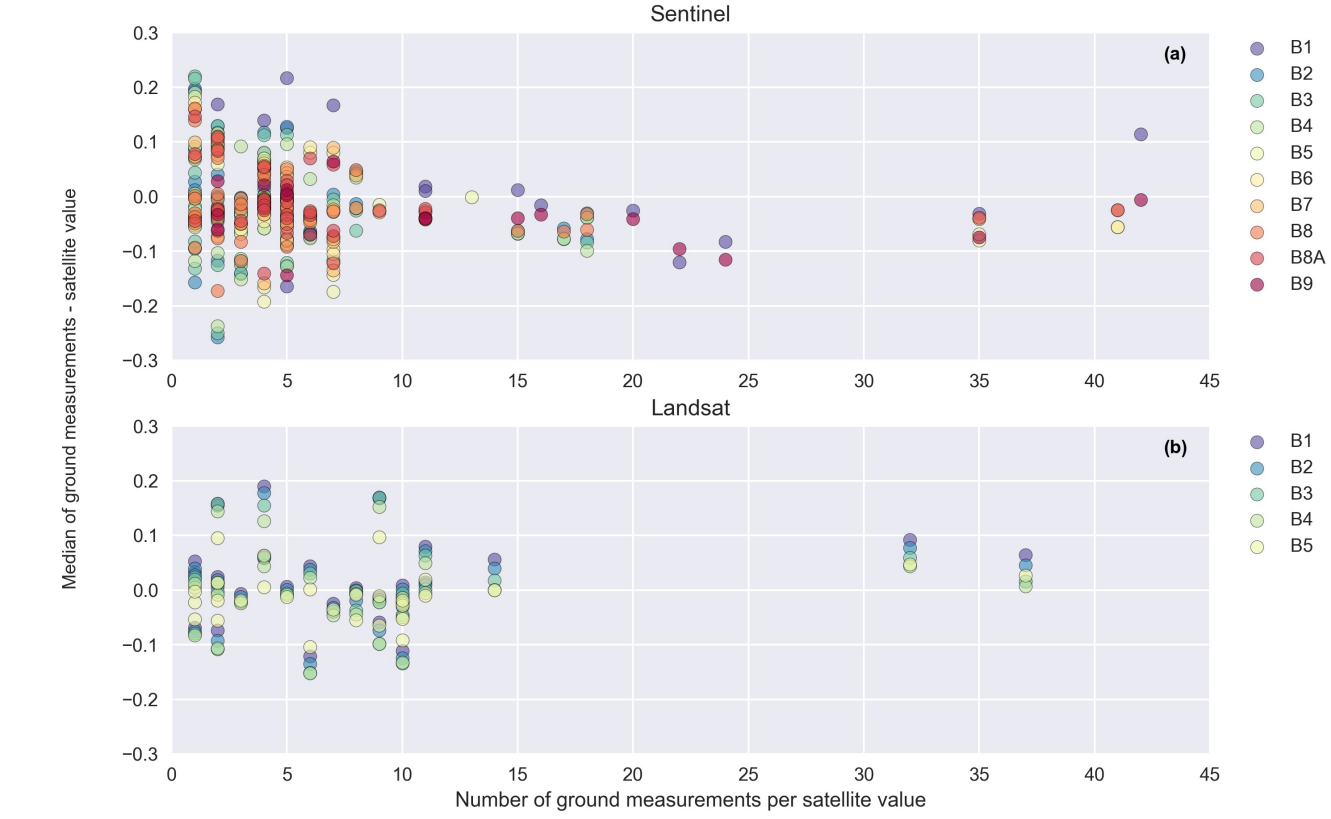

Figure 10: The number of ground measurements per unique satellite value (x-axis) is plotted against the difference between the median of these ground measurements in the respective wavelength band and the corresponding satellite value (y-axis). i.e. values that are positive in the vertical axis represent cases where ground reflectance is higher than satellite derived reflectance, whereas negative values represent the opposite. Different colours represent the different satellite bands, as indicated by the legend next to the plots.

https://doi.org/10.5194/tc-2020-92
Preprint. Discussion started: 21 April 2020

The Cryosphere
Discussions
Open Access
EGU

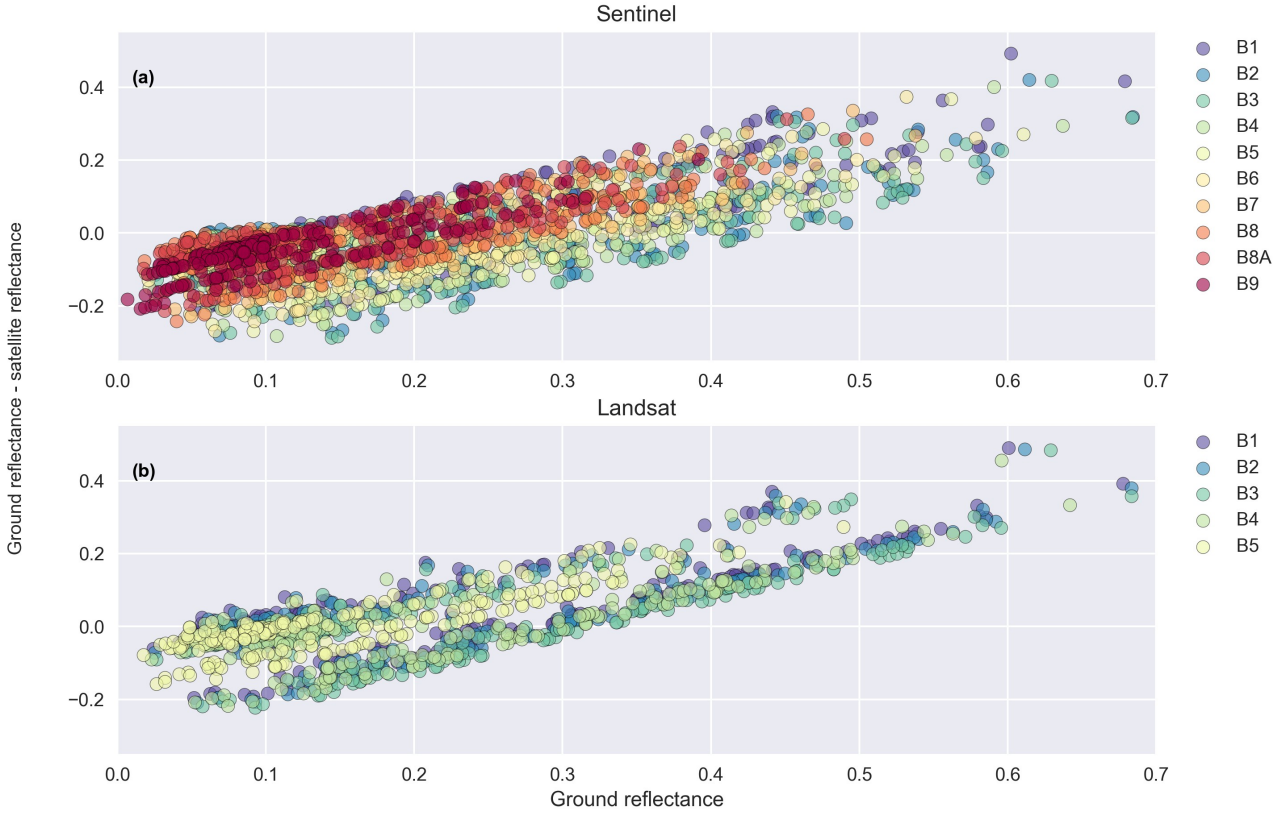

Figure 11: Same data as in Fig. 10, but showing individual sampling points without grouping by common satellite pixels.

https://doi.org/10.5194/tc-2020-92
Preprint. Discussion started: 21 April 2020

The Cryosphere
Discussions
Open Access
EGU

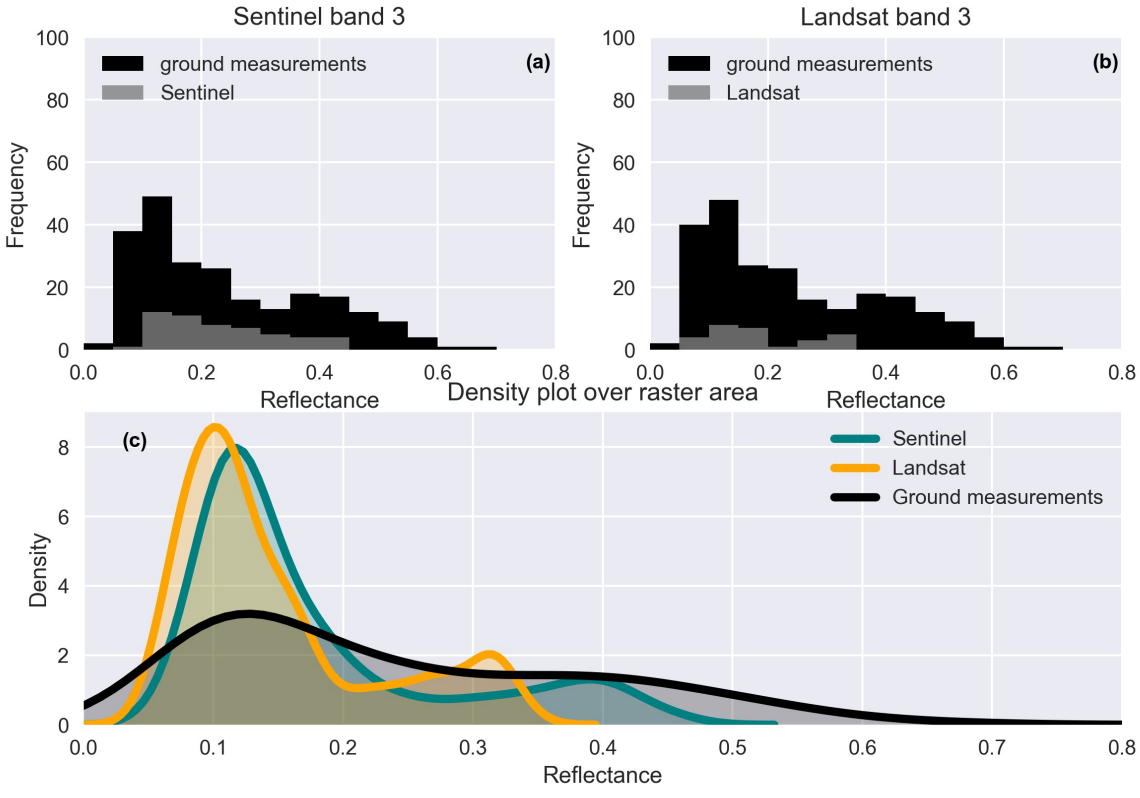

Figure 12: The histograms in the top panels (a, b) show the frequency of occurrence of the band 3 mean values of the ground measurements per reflectance bin. Bin width: 0.05. Overlaid in grey are the histograms of the corresponding satellite pixel values. The bottom panel (c) shows density plots of the Sentinel and Landsat band 3 rasters over the study area (smallest possible rectangle containing all ground measurements), with the density of the ground reflectance for comparison.

https://doi.org/10.5194/tc-2020-92
Preprint. Discussion started: 21 April 2020

Table 1: Literature overview on bare ice albedo measurements

Glacier	Albedo type	Temporal resolution	Spatial resolution	Reference
Hintereisferner, AT	Total	Multiple days	Multiple points on different surface types	Dirmhirn and Trojer, 1955.
Hintereisferner, AT	Total	Multiple times on one day	2 points	Jaffé, 1960.
Northern China (glacier not specified)	Spectral	Not specified	Different surfaces	Zeng et al., 1984.
Forbindels, Greenland	Spectral	One measurement campaign	Regular grid of points around multiple study sites	Hall et al., 1990.
Hintereisferner, AT	Spectral	7 days during ablation season	Points along a profile	Van de Wal et al., 1992.
Austre Brøggerbreen, Midre Lovénbreen, Svalbard	Spectral, total shortwave	Multiple days during ablation season	1 point	Winther, 1993.
Haut Glacier d'Arolla, CH	Total	One measurement campaign	Multiple points	Knap et al., 1999.
Chhota Shigri, Mera Glaciers, Nepal	Total shortwave	Continuous AWS measurements	AWS location	Brun et al., 2015.
Forni Glacier, IT	Total	Multiple measurements during multiple years	Multiple points	Azzoni et al., 2016.
Glacier de la Plaine Morte, CH	Spectral	One measurement campaign	Multiple points	Naegeli et al., 2015.
Findelen, CH	Total	Continuous AWS measurements	AWS location	Naegeli et al., 2017.
Morteratsch, CH	Spectral	One measurement campaign	Multiple points	Di Mauro et al., 2017.
Jamtal, AT	Spectral	One measurement campaign	Multiple points	This study

https://doi.org/10.5194/tc-2020-92
Preprint. Discussion started: 21 April 2020

Table 2: Description of the surface characteristics along each profile line, as well as number of spectra collected along the line and number of pixels intersected by the line in band 3 of the Sentinel and Landsat scenes, respectively.

	Qualitative description	Spectra	Sentinel B3 pixels	Landsat B3 pixels
P2	Relatively smooth, uniform ice surface, slightly wet.	11	3	2
P3	Mostly dry surface, clean cryoconite.	11	4	1
P4	Mostly dry ice surface, some dirt, some rocks/debris on ice surface where profile approaches moraine.	11	4	2
P5	Significant debris cover along profile. Where ice is exposed, ice surface is wet. Profile crosses meltwater channels with running water.	11	3	1
P6	Wet ice surface with dust/dirt transitions to cleaner, brighter ice.	11	4	1
P7	Grey-ish ice surface with meltwater channels and fine grained debris/small rocks.	11	2	2
P8	Similar to P7, fewer rocks.	11	4	2
P9	Wet ice surface with mixture of relatively clean cryoconite and more dusty areas.	11	3	2
P10	Wet ice surface with several small melt water channels. Mostly dirty, grey ice.	11	3	2
P11	Wet ice surface with several small meltwater channels. Very dirty ice with scatteredsmall rocks.	11	4	2
P12	Relatively clean, bright ice interspersed with larger meltwater ponds/channels, which contain dirt and small rocks.	11	4	3
P13	Clean cryoconite with some darker patches.	40	5	2
P14	Wet ice surface with fine grained dirt in relatively uniform cryoconite.	11	4	2
P15	Uneven ice surface, mostly clean, dry ice.	40	3	2
P16	Mixture of wet and dry ice surface and fine grained dirt.	11	3	2
P17	Mostly wet ice surface, fine grained dirt with some cleaner patches.	11	2	2

https://doi.org/10.5194/tc-2020-92
Preprint. Discussion started: 21 April 2020

445 **Table 3: Band names and respective wavelength range and resolution for Landsat and Sentinel as used in this study. Pearson correlation given for mean band values of ground-measurements and associated satellite data.**

	Landsat		
Band	**Range (nm)**	**Resolution (m)**	**Pearson Corr.**
1 (Coastal/Aerosol)	430-450	30	0.62
2 (Blue)	450-510	30	0.61
3 (Green)	530-590	30	0.58
4 (Red)	640-670	30	0.57
5 (NIR)	850-880	30	0.53
	Sentinel		
1(Coastal/Aerosol)	433-453	60	0.46
2 (Blue)	457.5-522.5	10	0.65
3 (Green)	542.5-577-5	10	0.63
4 (Red)	650-680	10	0.61
5 (Vegetation Red Edge)	697.5-712.5	20	0.57
6 (Vegetation Red Edge)	732.5-747.5	20	0.56
7 (Vegetation Red Edge)	773-793	20	0.55
8 (NIR)	784.5-899.5	10	0.56
8A (NIR narrow band)	855-875	20	0.53
9 (Water vapour)	953-955	60	0.3